ASPS Conference Proceedings 1: 875-883 (2022)

Proceedings of

12th Structural Engineering Convention-An International Event (SEC 2022)

Available at https://asps-journals.com/index.php/acp

Behaviour of Cold Formed Steel Rectangular Hollow Section Filled with Concrete under Cyclic Lateral Loadwith Constant High Axial Compression

R. Velmurugan[1,*], S.R. Satish Kumar[2]

[1]Department of Civil Engineering, MS Research Scholar, Indian Institute of Technology, Madras, 600 036, India
[2]Department of Civil Engineering, Professor, Indian Institute of Technology, Madras, 600 036, India

Paper ID - 060428

Abstract

This paper presents an experimental investigation of Rectangular Concrete Filled Steel Tube (RCFST) sections subjected to cyclic lateral load combined with constant high axial compression. A total of eight RCFST columns with different combinations of width to thickness ratio, slenderness ratio and axial compression ratio were tested. The constant axial compressive load on the test columns was 60% and 80% of its axial load carrying capacity. Failure modes such as local buckling and rupture of steel tube were observed from experiments during strength degradation after reaching maximum lateral load. From the experimental results, envelope curves were obtained by joining the locus of extremities of the load-displacement hysteresis loops. Seismic parameters such as strength, stiffness, ductility, and energy dissipation capacity were discussed based on experimental results.

Keywords: concrete filled steel tube, high axial compression, cyclic lateral load, seismic parameters, strength, ductility, energy dissipation.

1. Introductio

A concrete-filled steel tube (CFST) column consists of a steel tube filled with concrete. Furlong [1] reported that the concrete core adds stiffness and compressive strength to the tubular column and reduces the potential for inward local buckling. On the other hand, the steel tube acts as longitudinal and lateral reinforcement for the concrete core helping it to resist tension, bending moment, and shear and helping to prevent the concrete from spalling. Due to the benefit of composite action of the two materials, the CFT columns provide excellent seismic event resistant structural properties such as high strength, high ductility and large energy absorption capacity.

Elchalakani et al. [2] presented an experimental investigation of the flexural behavior of circular CFT subjected to large deformation pure bending where d/t = 12 to 110 and compared the behavior of empty and void-filled, cold-formed circular hollow sections under pure plastic bending.To investigate the seismic behaviour of concrete in-filled steel tube(CFT) columns, many quasi-static cyclic loading tests have been carriedout in the past, such as Sakino and Tomii [3], Nakaharaet al. [4], Nakanishi et al. [5], Elremaily and Aziznamini [6], Xiao et al. [7], Marson and Bruneau [8], Amir fam et al. [9], Kingsley et al. [10], Yaochun Zhang et al.[11], Han et al [19], Hajjar et al [16].

Varma et al [12] investigated about the level of axial load on the behaviour (stiffness, strength, ductility, and energy dissipation) of high strength square CFT beam columns. Roeder et al [21] did experimental research in CFST bridge columns and reported that CFST system is more resilient than the reinforced concrete (RC) system. Huang et al [22] investigated CFST truss girders and reported that concrete compressive strength has negligible effects on the failure mode of CFST truss girders. The majority of these investigations, however, have dealt with axially loaded columns. Comparatively, a very little work has been done on the columns subjected to axial load combined with lateral load, particularly, in the concrete filled rectangular steel tubular columns. There is a clear need to study the hysteretic behaviour of cold formed steel rectangular section filled with concrete.

In this paper, a detailed experimental study on RCFST columns subjected to cyclic lateral load combined with high axial load to study about seismic parameters such as strength, stiffness, ductility, energy dissipation from hysteretic and envelope curves.

2. Experimental Investigation

2.1 General

In this study, a total of 8 RCFST columns of length 1.5m were prepared. The main parameters varied in the columns were: (i) ratio of tube width to wall thickness, D/t (from 22 to 35), (ii) length to least radius of gyration of tube, L/r (from 40 to 60) and (iii) axial load to axial strength, axial compression ratio, n = P/Pc (from 0.6 and 0.8). Cross sectional details of RCFST column is shown in Fig. 1.

*Corresponding author. Tel: +918939746247; E-mail address: vrvelmurugan@gmail.com

Published online: December 19, 2022
doi:10.38208/acp.v1.596

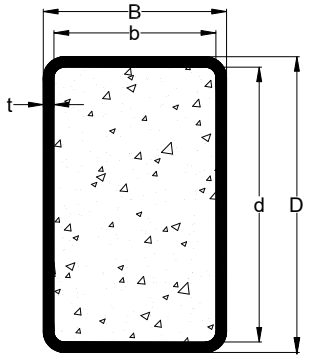

Fig. 1. Cross sectional details of RCFST

Table-1. Details of columns and Axial load capacity

Column	D mm	B mm	t mm	D/t	L/r	P_y kN	P_{cr} kN	P_c kN	P kN
C1-0.8P	145	82	5.4	26.29	44.83	1106	745	518	414
C1-0.6P	145	82	5.4	26.29	44.83	1106	745	518	311
C2-0.8P	145	82	4.8	30.21	44.51	1039	697	485	388
C2-0.6P	145	82	4.8	30.21	44.51	1039	697	485	291
C3-0.8P	122	61	5.4	22.59	60.71	800	302	239	192
C3-0.6P	122	61	5.4	22.59	60.71	800	302	239	144
C4-0.8P	122	61	3.6	33.88	59.01	639	240	190	152
C4-0.6P	122	61	3.6	33.88	59.01	639	240	190	114

A summary of details of the columns is presented in Table 1. Columns C1-0.8P was named such that, C-denotes column, 1- denotes first type of cross section based on D/t ratio and 0.8 denotes axial load ratio. Similarly, in C2-0.6P,C-denotes column, 2- denotes second type of cross section and b/t ratio and 0.6 denotes axial load ratio. Allcolumns were named using the similar notation.

2.1 Material Properties

The steel tubes used for the fabrication of columns were made of YST310 Grade steel. The mechanical properties of the YST310 Grade steel are summarized in Table 2.

Self-Compacting Concrete (SCC) was used to fill the steel tubes. The cube compressive strength of SCC was found by preparing 10-trial mixes. The parameters varied in trial mix were cement, fly ash, water powder ratio, size of coarse aggregate and superplasticer (Glenium B233) content. For each trial of concrete mix, nine 150 mm cubes were casted and cured to find cube compressive strength (f_{ck}) on third, seventh and twenty eighth dayafter casting. Finally, a trail mix was selected based on the strength (40MPa) and result from slump flow test (slump flow diameter was approximately 600mm).

Table-2. Mechanical properties of YST 310 Grade Steel

Elastic Modulus (E_s)	2.1 x 10^5 MPa
Yield stress (f_y)	310 MPa
Ultimate tensile stress (f_u)	450 MPa

2.2 Preparation of Columns

Steel tubes were cut for required length and welded with gusset plates and base plate at column bottom to ensure a strong connection. After fabrication, the tubes were filled with SCC and kept for 28 days before starting experimental investigation.

2.3 Prediction of Axial Strength of RCFST column

Table-1 shows axial strength and axial load to be applied on all the columns to be tested are calculated using formula based on Ben Kato [20]. The axial load to be applied on the RCFST column is

$$P = 60\%\ and\ 80\%\ of\ P_c$$

The buckling strength of centrally loaded columns, P_c, could be given by the general form as

$$P_c = gP_y \quad (1)$$

where,

g = reduction coefficient in terms of relatives lenderness $\bar{\lambda}$

$$= \alpha\left(1 - \sqrt{1-\beta}\right) \quad (2)$$

$$\alpha = \frac{1 + 0.34\left(\bar{\lambda} - 0.2\right) + \bar{\lambda}^2}{2\bar{\lambda}^2} \quad (3)$$

$$\beta = (\alpha * \bar{\lambda})^{-2} \quad (4)$$

$\bar{\lambda}$ = relative slenderness ratio of the column

$$= \sqrt{\frac{P_y}{P_{cr}}}$$

$$= \sqrt{\frac{A_s f_y + A_c f_{ck}}{\left(\frac{\pi^2(E_s I_s + E_c I_c)}{(kL)^2}\right)}}$$

$$= \frac{kL}{\pi}\sqrt{\frac{A_s f_y + A_c f_{ck}}{E_s I_s + E_c I_c}} \quad (5)$$

P_y = squash load (maximum compressive strength which is not influenced by stability)

$$= A_s f_y + A_c f_{ck} \quad (6)$$

P_{cr} = Eulerian elastic buckling strength

$$= \frac{\pi^2(E_s I_s + E_c I_c)}{(kL)^2} \quad (7)$$

f_y = yield strength of steel

f_{ck} = characteristic strength of concrete

E_s = modulus of elasticity of steel

E_c = modulus of elasticity of concrete

L = length of column

k = effective length factor

= 2 for cantilever column

B = outer breadth of the RCFST section (perpendicular to minor axis)

D = outer depth of the RCFST section (perpendicular to major axis)

b = inner breadth of the RCFST section (perpendicular to minor axis)

d = inner depth of the RCFST section (perpendicular to major axis)

A = cross sectional area of the RCFST section

A_c = cross sectional area of the concrete section

A_s = cross sectional area of the steel section

I_c = moment of inertia of the concrete section (about minor axis)

I_s = moment of inertia of the steel section (about minor axis)

2.4 Prediction of Lateral yield displacement about minor axis

Fig. 2 shows the transformed section of RCFST. Breadth of steel equivalent to concrete is

$$d_e = \frac{A_{se}}{b} \tag{8}$$

For a beam, the yield stress f_y and bending moment M_y are related by the equation

$$M_y = \frac{f_y}{y} * I \tag{9}$$

where,

I = moment of inertia of the transformed section

y = depth of extreme fibre from neutral axis

Lateral yield load [15], [18] of a column with axial load P is taken as the smaller one from Eqn (10) and (11)

$$H_y = \frac{M_y}{0.85 * h}\left(1 - \frac{P}{P_E}\right)\left(1 - \frac{P}{P_u}\right) \tag{10}$$

$$H_y = \frac{M_y}{h}\left(1 - \frac{P}{P_y}\right) \tag{11}$$

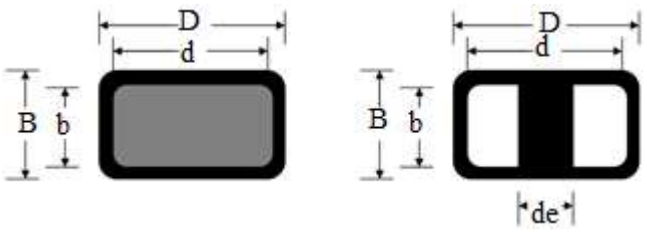

Fig. 2. Transformed Section RCFST

where M_y = yield moment of cross section

P_E = Euler's buckling load of a cantilever column

P_u = ultimate strength of centrally loaded column

Lateral yield displacement of column is given by

$$\Delta_y = \frac{H_y h^3}{3EI} \tag{12}$$

Theoretically calculated yield lateral load and displacement are listed in Table 3.

2.5 Test setup and instrumentation

Test setup and schematic diagram of test setup of the column is shown in the Fig.3 and Fig.4 respectively. Fabricated RCFST column was placed on the rigid beam anchored rigidly with floor of the laboratory. The base plate of the column was connected with rigid beam as it gives fixed end connection. Hydraulic Actuator was positioned horizontally in such a way that one end of the actuator is connected with rigid frame and other end is connected with top of the column. In-plane cyclic lateral loads were applied by Hydraulic Actuator attached to the top of the column.

Hinged-Rigid-Sliding arrangement of Hydraulic Jack is shown in Fig. 5. Hydraulic Jacks positioned vertically on Hinged-Rigid-Sliding arrangement, were used to apply axial compressive load to the columns. The hydraulic jacks were monitored for maintaining uniform pressure, thereby ensuring constant axial load on the top of the column. A 'Teflon sheet sliding' arrangement was provided for free in plane movement of the Hydraulic Jack with rigid beam.

Table-3. Predicted yield lateral load and displacement

Column	M_y kNm	H_y kN	Δ_y mm
C1-0.8P	24.45	1.70	2.82
C1-0.6P	24.45	4.47	7.41
C2-0.8P	22.87	1.59	2.82
C2-0.6P	22.87	4.18	7.40
C3-0.8P	13.33	0.77	3.13
C3-0.6P	13.33	2.19	8.96
C4-0.8P	10.59	0.61	3.12
C4-0.6P	10.59	1.74	8.95

Fig. 3. Test setup of column

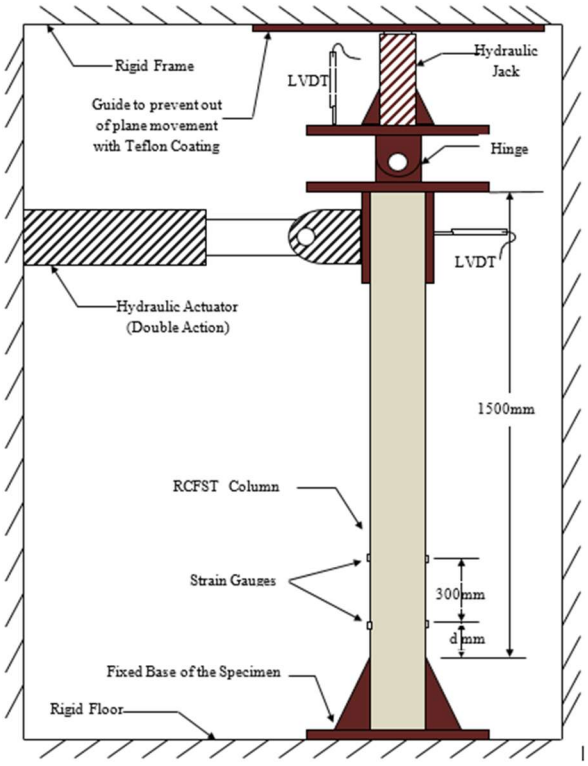

Fig. 4. Schematic diagram of test setup

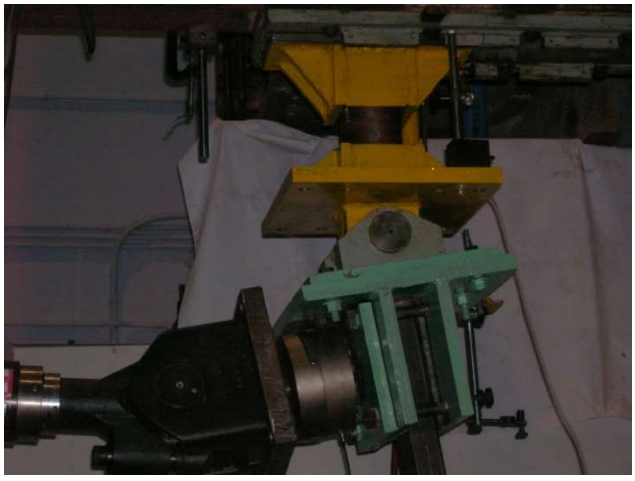

Fig. 5. Hinged-Rigid-Sliding arrangement of Hydraulic Jack

Fig. 6. Location of strain gauges at base of column

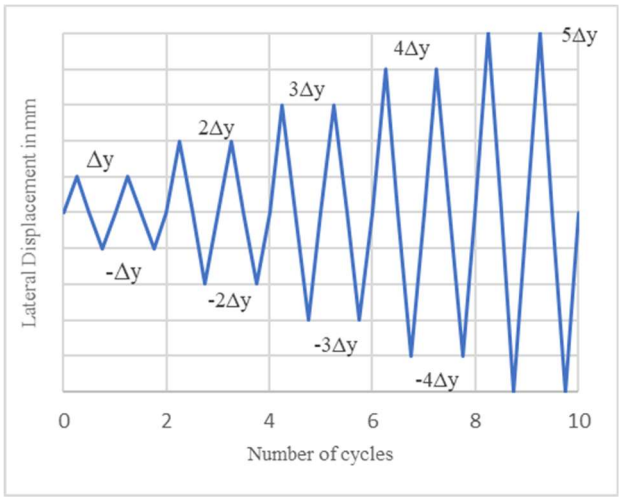

Fig. 7. Cyclic lateral displacement protocol

Two LVDT's were placed to measure the deformation of the column, first one was placed vertically with hydraulic jack frame to measure the axial deformation of the column and the second one was placed horizontally with hydraulic actuator to measure the lateral displacement of the top of the column. Location of the LVDT are shown in Fig.4.

Strain gauges were placed at the bottomof the column to measure the strains. Four strain gauges were placed on one face of the column, out of whichthree were placed at height of 'd' and the fourth one was placed at (d + 300) mm from the base of the column, where d is equal to longest straight edge width of the column. Similarly, another four strain gauges were placed on another face of the column. Location of the strain gauges are shown in Fig.6. Measurements from LVDT and Strain Gauges were recorded using data acquisition system.

2.6 Test Procedure

The targeted axial load was applied to the column using Hydraulic Jack and maintained constantly throughout the experiment. The in-plane cyclic lateral load was applied at the top of the column using hydraulic actuator by displacement control method.The loading history adopted for column is shown in Fig. 7. Yield displacement(Δ_y) value for the column from Table-3 was used for applying the lateral displacement. The amplitude of incrementally increasing cyclic lateral displacement was taken as Δ_y, $2\Delta_y$, $3\Delta_y$, $4\Delta_y$ etc., up to failure column.

Simultaneously the strain gauges and LVDT readings were measured using the data acquisition system.Experiment was stopped, when occurrence of some visible failure and load carrying capacity of the column was dropped around 30 to 40% of the peak load.

3. Analysis of experimental results

3.1. Failure modes

Fig.8 shows failure modes at different amplitudes of lateral displacement. Failure mode was not visible anywhere in the column up to peak lateral load. After reaching peak load, a slight outward local buckling of steel tube was visible near the base of almost all columns in face

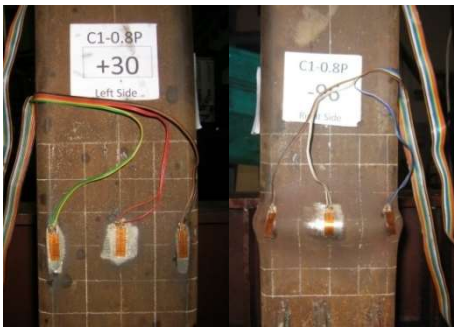

(a) Failure is not visible (b)outward local buckling

(c)Increasing outward local buckling of steel tube

(d) Finally - rupture of steel tube

Fig. 8. Failure mode - outward local buckling of columns

perpendicular to the loading direction. With additional cycles, buckling progressed on opposite faces of the column followed by gradual strength and stiffness degradation was observed. Finally, outward local buckling formation in all four sides were clearly visible and rupture of steel tube was occurred in additional cycles.

Global buckling mode of failure was observed in column C3-0.8P after reaching peak load. This column was failed in different manner while comparing to all the other columns. Fig. 9 shows global buckling mode of column.

3.2. Hysteretic and Envelope curve of lateral load – lateral displacement

Fig. 10shows the observed lateral load–lateral deflection hysteretic curves and envelope curves of all RCFST columns subjected to cyclic lateral loading combined with constant axial load. The envelope curves of the tested columns shown in Fig.10 were constructed by connecting the maximum load point at each displacement level according to

Fig. 9. Failure mode - Global buckling of column C3-0.8P

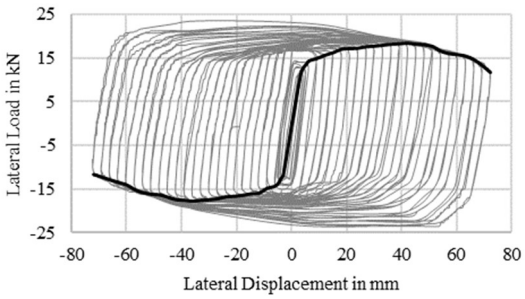

(a) C1-0.8P

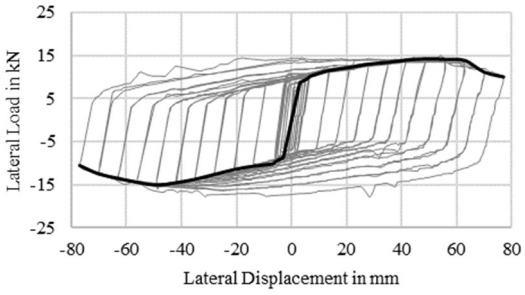

(b) C1-0.6P

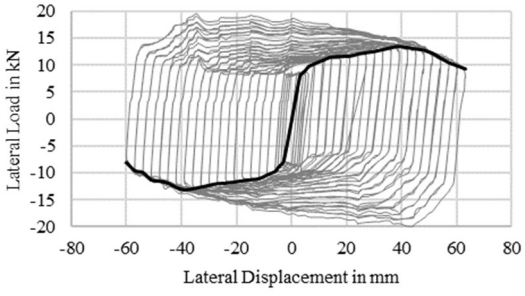

(c) C2-0.8P

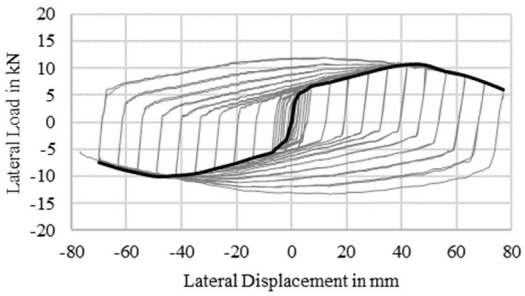

(d) C2-0.6P

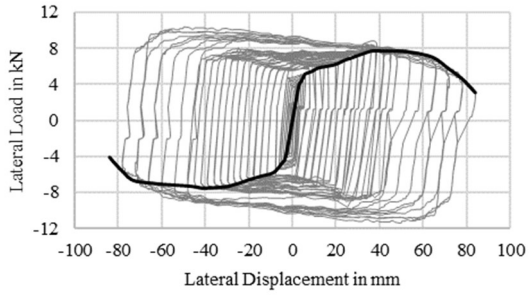

(e) C3-0.8P

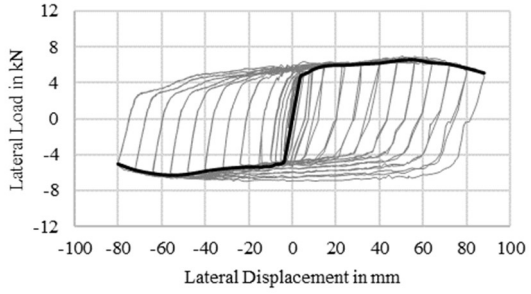

(f) C3-0.6P

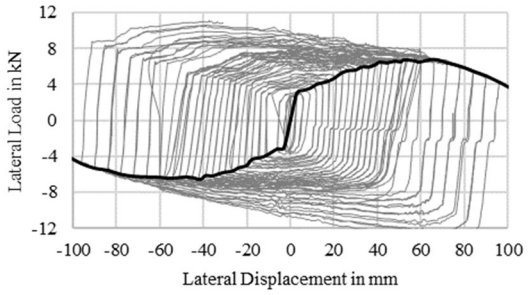

(g) C4-0.8P

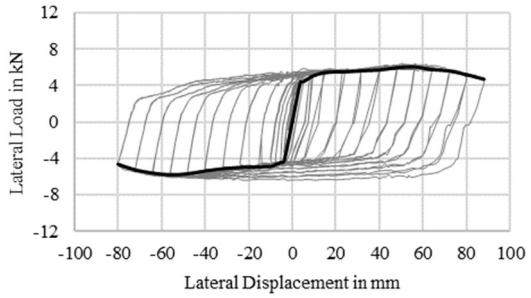

(h) C4-0.6P

Fig. 10. Hysteretic Curve and Envelope Curve of Lateral Load and Lateral Displacement

the lateral load–lateral displacement hysteretic curves. Envelope curve obtained from hysteretic curve is almost same for push and pull lateral load on the column. These curves indicate that an inelastic response occurred from initial loop onwards for all columns and subsequently the columns entered the elastoplastic process accompanied by gradual stiffness degradation and energy dissipation. A gradual decline in strength could be observed when the maximum lateral load was reached. Table-4 shows that the peak lateral load decreases with decrease in axial compression ratio.

3.3. *Ductility*

In order to evaluate accurate information on the ductility of columns, displacement ductility ratio$\mu_y$based on yield point and displacement ductility ratio $\mu_m$based on peak point was calculated by

$$\mu_y = \frac{\delta_u}{\delta_y} \tag{13}$$

$$\mu_m = \frac{\delta_u}{\delta_m} \tag{14}$$

where δ_u , δ_m and δ_y are lateral displacement at ultimate (failure), maximum (peak) and yield point in envelope curve. Because there was not an apparent yield point on the envelopes of hysteretic curves, δ_u , δ_m and $\delta_y$cannot be directly obtained from the above curves. In this study general yield moment method [13],[14],[17] was adopted to obtain the yield point and ultimate point in envelope curve. This method depicted in Fig. 11, in which point (δ_m,H_m) is the peak point (M) determined by the maximum lateral load, the ultimate failure point (U) is defined as point (δ_u,H_u) where δ_u is the lateral displacement when the load decreases to$H_u = 0.85H_m$and theyield (Y) point(δ_y,H_y)was determined as explained below. The tangent to envelope curve at origin O and peak point M intersects at point A. Vertical line drawn at point A meets the envelope curve at point B. Line connecting origin O and B meets tangent M at point C. Vertical line drawn at point C meets the envelope curve at yield point Y.

It was found that the position of yield point was influenced by the amplitude of initial cycle. Table 4 shows that the ductility μ_y varies from 5.52 to 11.54 and μ_m varies from 1.29 to 1.57. Table 4 shows that μ_y increases with decrease of axial compression ratio for all column except column C2 and μ_m decreases with increase of axial compression ratio.

Table-4. Displacement ductility ratio

Column	δ_y mm	δ_m mm	δ_u mm	H_y kN	H_m kN	H_u kN	μ_y	μ_m
C1-0.8P	7	41.5	61	14.5	18.3	15.56	8.71	1.47
C1-0.6P	7.5	50	67	10.5	14.4	12.24	8.93	1.34
C2-0.8P	7	39	53	10	13.5	11.48	7.57	1.36
C2-0.6P	10.5	45	58	6.75	10.8	9.18	5.52	1.29
C3-0.8P	9	38.5	56.5	5.5	7.75	6.59	6.28	1.47
C3-0.6P	6.8	54.5	78.5	5.1	6.7	5.70	11.54	1.44
C4-0.8P	12.5	52	81.5	4	6.75	5.74	6.52	1.57
C4-0.6P	7.5	55	81	4.9	6.2	5.27	10.80	1.47

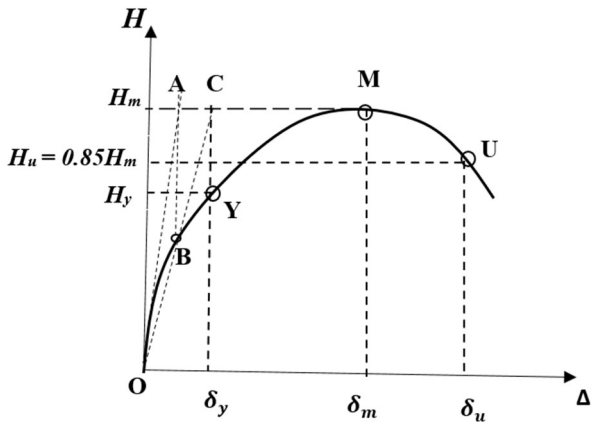

Fig. 11. General yield moment method

3.4. *Stiffness degradation*

During cyclic loading, the RCFST columns experienced progressive stiffness degradation. The secant stiffness for each cycle is obtained from the ratio between peak load and peak displacement for that cycle. Fig. 12 shows the patterns of secant stiffness degradation for all RCFST columns. The secant stiffness of column degrades from initial cycle of lateral displacement onwards.

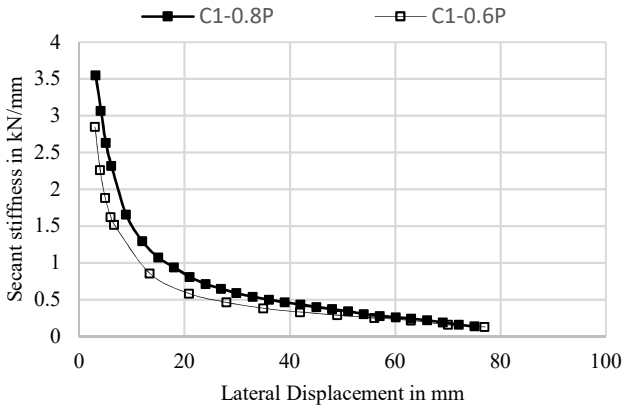

(a) C1

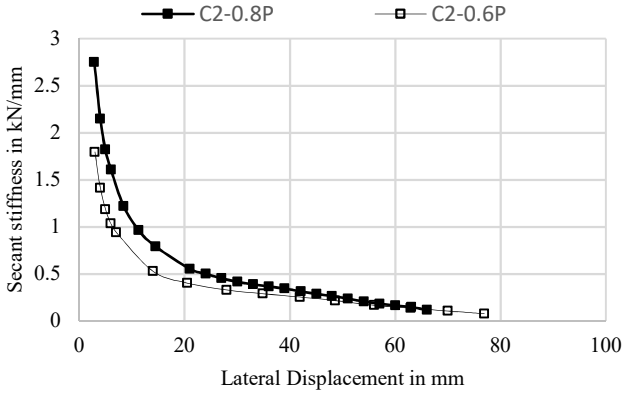

(b) C2

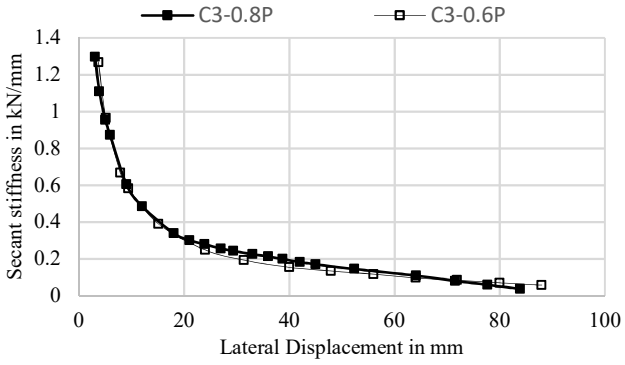

(c) C3

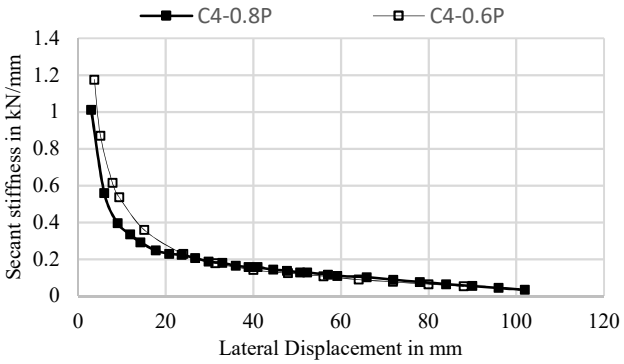

(d) C4

Fig. 12. Stiffness degradation

3.5. *Energy dissipation capacity*

The transformation of mechanical properties for RCFST columns under an earthquake is accompanied with the energy dissipation, determining whether the structure can resist the earthquake motion. In this study, an energy dissipation analysis was conducted through the area integral based on the hysteretic loops. Moreover, the results of the accumulated energy ratio analysis and ultimate energy analysis can be observed in Fig. 13 and 14, respectively.

The accumulated energy ratio could be calculated as follows

$$R_{Ei} = \sum_{i=1}^{n} E_i / E_T$$

where,E_i is the accumulated energy until the nth cyclic loop, and E_T isthe total ultimate energy dissipation.

Fig. 13 shows the result of the accumulative energy ratio analysis, indicating that the cumulative damage developed in nonlinearly from initial loop on wards. For the convenience of unified comparison, using the total dissipated energy until peak point as the ultimate energy dissipation, the ultimate energy analysis of all tested columns was investigated, as shown in Fig. 14. It indicates that the columns with 80% axial load dissipates more energy than the column with 60% axial load.

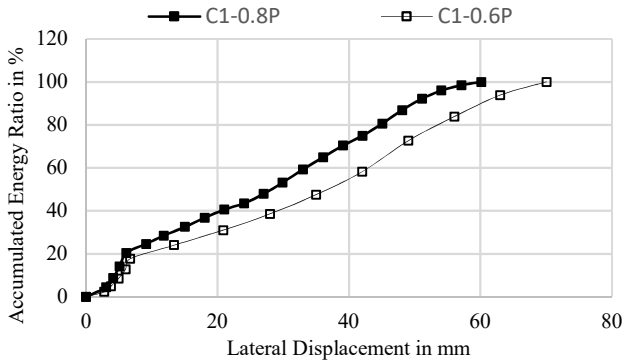

(a) C1

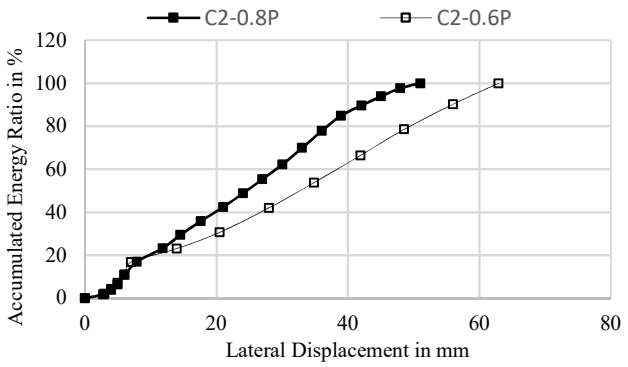

(b) C2

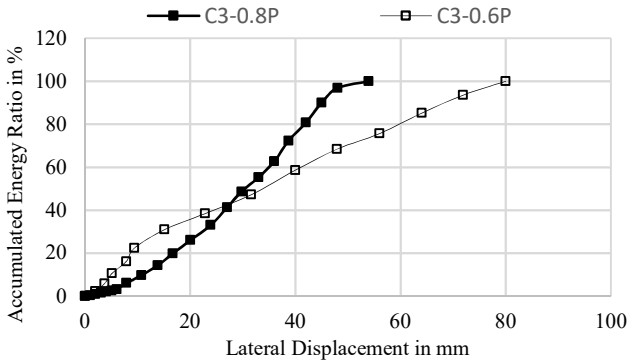

(c) C3

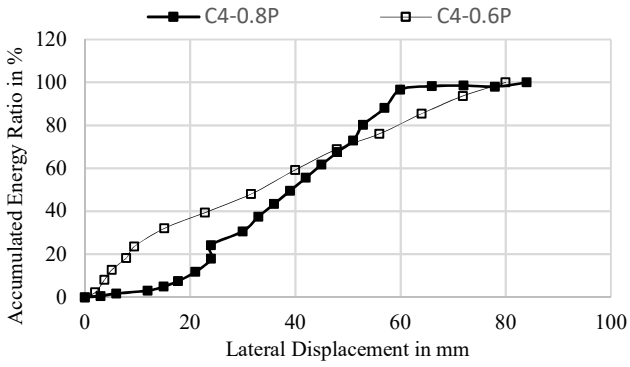

(d) C4

Fig.13. Accumulated Energy Ratio

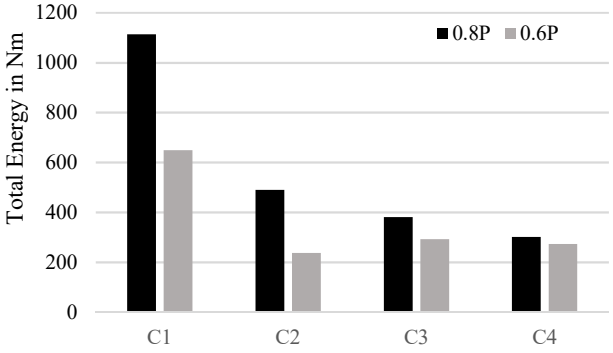

Fig. 14. Total energy analysis

4. Summary and Conclusions

This paper presented the results of an experimental study on Rectangular Concrete Filled Steel Tube (RCFST) sections subjected to cyclic lateral load combined with constant high axial compression. A total of eight RCFST columns with different combinations of width to thickness ratio, slenderness ratio and axial compression ratio were tested. Based on the experimental results, the following conclusions are drawn within the scope of the current study:

1. Failure mode was not visible anywhere in the column up to peak lateral load. After reaching peak load, a slight outward local buckling of steel tube was visible near the base of column in compression face, then local buckling formed in all faces and finally rupture was occurred in locally buckled steel tube. Global buckling mode of failure was observed in column C3-0.8P after reaching peak load.
2. Envelope curve obtained from hysteretic curve is almost same for push and pull lateral load on the column.
3. The peak lateral load decreases with decrease in axial compression ratio.
4. The position of yield point was influenced by the amplitude of initial cycle of lateral displacement. Displacement ductility based on yield point, μ_y varies from 5.52 to 11.54 and Displacement ductility based on peak point, μ_m varies from 1.29 to 1.57. It was observed that μ_y increases with decrease of axial compression ratio for all column except column C2 and μ_m decreases with increase of axial compression ratio.
5. The secant stiffness of column degrades from initial cycle of lateral displacement onwards.
6. Energy dissipation starts from initial cycle of lateral displacement and it progresses up failure point. Columns with 80% axial load dissipates more energy than the column with 60% axial load

Disclosures

Free Access to this article is sponsored by SARL ALPHA CRISTO INDUSTRIAL.

References

1. Furlong, R.W. (1967), “Strength of Steel-Encased Concrete Beam-Columns,” Journal of Structural Division, ASCE, 93(ST5), 113–124.
2. M.Elchalakani, X. L. Zhao, and R. H. Grzebieta, “Concrete-filled circular steel tubes subjected to pure bending,” Journal of Constructional Steel Research, vol. 57, no. 11, pp. 1141–1168, 2001.
3. Sakino K, Tomii M. Hysteretic behavior of concrete filled square steel tubular beam-column failed in flexure. Trans JpnConcr Inst 1981;3:439–46.
4. Ninakawa, Nakahara, Sakino. Cyclic bending behavior of concrete filled steel tubular columns under constant gravity load. J Struc Constr Eng AIJ 2003;568:139–46.

5. Nakanishi Katsuyoshi, Kitada Toshiyuki, Nakai Hiroshi. Experimental study on ultimate strength and ductility of concrete filled steel columns under strong earthquake. J Constr Steel Res 1999;51:297–319.
6. Elremaily A, Azizinamini A. Behavior and strength of circular concrete-filled steel tube columns. J Constr Steel Res 2002;58:1567–91.
7. Xiao Y, He WH, Mao XY. Development of confined concrete filled tubular (CCFT) columns. J Build Struct 2004;6:59–66.
8. Marson J, Bruneau M. Cyclic testing of concrete-filled circular steel bridge piers having encased fixed-based detail. J BridgEng ASCE 2004;1:14–23.
9. Fam Amir, Qie Frank S, Rizkalla Sami. Concrete-filled steel tubes subjected to axialcompression and lateral cyclic loads. J Struct Eng ASCE 2004;130:631–40.
10. Williams, Kingsley, Lehman, Roeder. Experimental investigation of column-tofooting connections for high-strength vanadium steel concrete-filled tube construction. Steel Struct 2005;5:377–87.
11. Zhang Yaochun, Chao Xu, Xiaozhe Lu. Experimental study of hysteretic behaviourfor concrete-filled square thin-walled steel tubular columns. J Constr Steel Res2007;63:317–25.
12. Varma AH, Ricles JM, Sause R, Lu LW. Seismic behavior and modeling of highstrength composite concrete-filled steel tube (CFT) beam–columns. J Constr SteelRes 2002;58(5–8):725–58.
13. P. Gajalakshmi, H. Jane Helena, Behaviour of concrete-filled steel columns subjected to lateral cyclic loading, Journal of Constructional Steel Research, Volume 75, 2012, Pages 55-63.
14. Jiantao Wang, Qing Sun, Junxin Li,Experimental study on seismic behavior of high-strength circular concrete-filled thin-walled steel tubular columns,Engineering Structures,Volume 182,2019,Pages 403-415.
15. Usami T, Ge H. Ductility of concrete-filled steel box columns under cyclic loading. JStruct Eng 1994;120(7):2021–40.
16. Hajjar JF, Gourley BC. A cyclic nonlinear model for concrete-filled tubes. I:Formulation. J Struct Eng 1997;123(6):736–44.
17. Zhou T, Chen Z, Liu H. Seismic behavior of special shaped column composed ofconcrete filled steel tubes. J Constr Steel Res 2012;75:131–41.
18. Ge H, Usami T. Cyclic tests of concrete-filled steel box columns. J Struct Eng1996;122(10):1169–77.
19. Han LH, Yang YF. Cyclic performance of concrete-filled steel CHS columns under flexural loading. J Constr Steel Res 2005;61(4):423–52.
20. Ben Kato, Column curves of steel-concrete composite members,Journal of Constructional Steel Research, Volume 39, Issue 2, 1996, Pages 121-135.
21. Roeder CW, Stephens MT, Lehman DE. Concrete filled steel tubes for bridge pier andfoundation construction. Int J Steel Struct 2017.
22. Huang, W., Lai, Z., Chen, B., Xie, Z., and Varma, A. H. (2018). “Concrete filled steel tube (CFT) truss girders: Experimental tests, analysis, and design.” Eng. Struct., 156(Feb), 118–129.